MATERIALE PLASTICE
https://revmaterialeplastice.ro
https://doi.org/10.37358/Mat.Plast.1964

Experimental and Numerical Evaluation of the Stress-strain Characteristic for Synthetic Rubber Spheres

ELENA SIRGHIE, ILIE MUSCA*, IONUT CRISTIAN ROMANU, IONUT MARIUS NAZARIE
"Ștefan cel Mare" University, Suceava, Faculty of Mechanical Engineering, Automotive and Robotics, 13 University Str., 720229, Suceava, Romania

***Abstract**: The paper presents a parallel between the calculation of deformations for uniaxially compressed rubber spheres, by direct measurement on the experimental stand. Generalities about rubber, definition, properties, main characteristics and examples of use, are presented. The authors' original experimental study is then presented to study the deformability of rubber spherical bodies and to analyze the deviations of rubber behavior from Hertzian model. An experimental rig was designed for this purpose. Its operation and the working method used, as well as the force-strain characteristics for different experimental situations (spheres'arrangement and support) are presented, that being the compression of two or three rubber spheres, with three different ways of supporting them. Considering that a model that accurately describes the behavior of rubber the spheres are made of is the Money-Rivlin model, which is characterized by two constants, C_{10} and C_{01}, these constants were determined by a simple method, using the hardness of the material as a basic element hyperelastic, measured on the Shore A scale. After determining the material constants, the deformation values were also determined by numerical modeling with the help of Ansys software. For validation, the experimental curve for the deformation of a rubber sphere on a plane and the numerical curve for the similar situation with the experimentally determined mechanical characteristics, were plotted on the same graph. Finally, the conclusions resulting from the conducted research are presented: - highlighting two ways of evaluating the deformation of rubber spheres, experimentally and numerically, determining the specific Mooney-Rivlin constants of the material through a simple, efficient and valid method, - a way to calculate deformations for this case of loading rubber spheres is to model them as an axisymmetric contact (reducing the model to a quarter), - by finite element method, because it uses a lower number of finite elements and saves significant resources,both the calculation method and the experimental methods used are validated by a good correspondence between the experimental curve and numerical results.*

***Keywords*:** *synthetic rubber, compression of spheres in contact, experimental methods, direct measurement, numerical modelling.*

1. Introduction

1.1. Overview

Synthetic rubbers are elastic materials, made by chemical processes from petroleum products. - They were developed to replace and improve the properties of natural rubber in the context of modern industrial and technological requirements.

Contemporary technology frequently uses rubbers due to their remarkable elasticity and durability. These characteristics makes rubbers indispensable structural materials in modern technology.

According to Treloar [1], the most important characteristic of rubber is its high deformation capacity, even under relatively small stresses. In the case of this material, the direct proportionality between stresses and strains does not hold and the stress-strain relationship is non-linear, making Hooke's law inapplicable Thus, a constant value can be assigned to the Young's modulus of elasticity only in the area where the deformations are small. In this area, the value of the modulus of elasticity is given by the tangent to the curve stress – strain, at the origin and is about 10^6 Pa, for rubber-like materials [1].

Materials with high elasticity and low modulus, as rubbers, differ significantly from ordinary solid materials, such as steel, which has a Young's modulus value of 2.1 10^{11} Pa.

**email: iliem@usm.ro*

Rubbers can deform 20-30 times more than steel, making them distinct from other materials, such as metals, plastics, abrasives, wood and leather. Also, the deformation of synthetic rubbers is completely reversible under the action of relatively small loads.

Rubbers have an extremely low volumetric compressibility and a high Poisson's ratio, ranging between 0.4 and 0.5, in contrast to the value of 0.28 for steel [2]. The exceptional capacity for elastic deformation and very high fatigue resistance for certain types of rubber is combined with a number of other valuable technical properties, such as:

-significant wear resistance,

-high friction coefficient, which sometimes remains constant even when the input parameters vary,

-tensile and impact resistance,

-good ability to resist to cuts,

-low density (from 0.95 10^3 kg m^{-3} to 1.6 10^3 kg m^{-3}).

Rubber hardness is an essential mechanical characteristic, which measures the stiffness of an elastic and isotropic material, reflecting its mechanical properties as well as other attributes, such as modulus of elasticity.

For rubbers and other polymers, the relationship between hardness and modulus of elasticity can vary depending on material composition, vulcanization process, and test conditions. In general, a harder rubber has a higher modulus of elasticity, which indicates a greater resistance to deformation under load [3].

Rubber resists better at compression loads than tensile ones, due to its molecular structure and the way its behaves under load.

1.2. Applications

Rubbers are highly adaptable materials and have a wide range of uses in various fields. Here are some examples:

- vehicles: rubber pads and dampers are essential to absorb shocks and reduce vibrations in cars, trucks and motorcycles, thus improving comfort and stability while driving; another common use for rubber is tires for cars, trucks, bicycles and other vehicles,
- industrial machines: In industrial equipment, rubbers are used to protect machines and operators from vibrations and shocks, extending the life of the equipment and ensuring smoother operation, but also for the manufacture of seals and protective bellows.
- buildings and structures: rubber buffers are used to isolate vibrations and noises, as well as to protect buildings from seismic movements, contributing to structural safety,
- appliances: in household appliances, such as washing machines and refrigerators, rubber pads help reduce noise and vibration, thus improving the operation quality.
-

1.3. Experimental studies degarding the behavior of rubber spheres used as seismic insulators

Katsamatas and collaborators [4] present an experimentally study on the behavior of a rolling, flexible seismic isolator, consisting of two concrete plates and a rubber sphere placed between them. The experimental investigation included uniaxial compression tests to characterize the response of the rubber spheres under normal load. Compression tests were performed using an universal testing machine under displacement control. Travel speeds were 0.0835 mm/s, 0.167 mm/s, and 0.33 mm/s. The results indicated that the tested spheres can withstand ~~to~~ a very high normal loads, with residual deformation. Rubber spheres with a diameter of 25 mm, 50 mm and 100 mm, with a Shore hardness of 85 A were used. The 25 mm spheres withstood a load of up to 3 kN, those with a diameter of 50 mm withstood 29 kN, and those with a diameter of 100 mm resisted up to 120 kN. In all cases, the compression test was manually stopped due to excessive deformation of the rubber isolators. The authors concluded that the force – deformation graphs for the tested spheres differ, because the material properties of the rubber spheres depend on their size. They observed that the material of the small spheres is stiffer, although they have the same hardness. It is noted that, for the range of characteristic stresses, calculated as F/D^2,

F being the force acting on the sphere and D – its diameter, used in the experiments, the 50 mm and 100 mm diameters spheres, in the range of 0.2–1.6 MPa, show relatively small difference between the normalized force-strain curves. It is important to note that the force-deformation curve, for small normalized deformations ($\delta/D < 0.2$), it is almost linear, contrary to the Hertz solution (where D - diameter of the deformed sphere [mm], F – the applied load [N], and δ – the deformation [mm]).

The high deformability of rubbers is essential in many industrial applications, often affecting the functionality of the equipment by changing the relative position of the elements. For this reason, it is important that deformations are controlled. The evaluation of their deformations' magnitude can be done either by direct measurement on experimental stands or by calculation, by different methods.

The experimental determination requires specific laboratory equipment, corresponding to the shape, dimensions and loading of the bodies. So, when this equipment is expensive or unavailable, the possibility of numerically estimating the deformations becomes important.

Also, the possibility to numerically estimate the response in deformations, allows for using it in the design phase, as part of the shape optimization, according to the operational requirements. In this sense, it is presented below a comparison of two methods for evaluating the deformations of rubber spheres, by actual measurement and by numerical modeling. Finally, the two obtained results, experimentally and numerically, are compared.

2. Materials and methods

2.1. Test rig for testing rubber spheres. Experimental methodology

To investigate the deformability of spherical rubber bodies under compression loads and to determine the relationship between compression load and the correlate deformation, as well as to analyze the behavior deviation of these materials from the Hertzian model, an experimental equipment was designed and realised [5, 6]. This equipment is presented in detail in Figure 1.

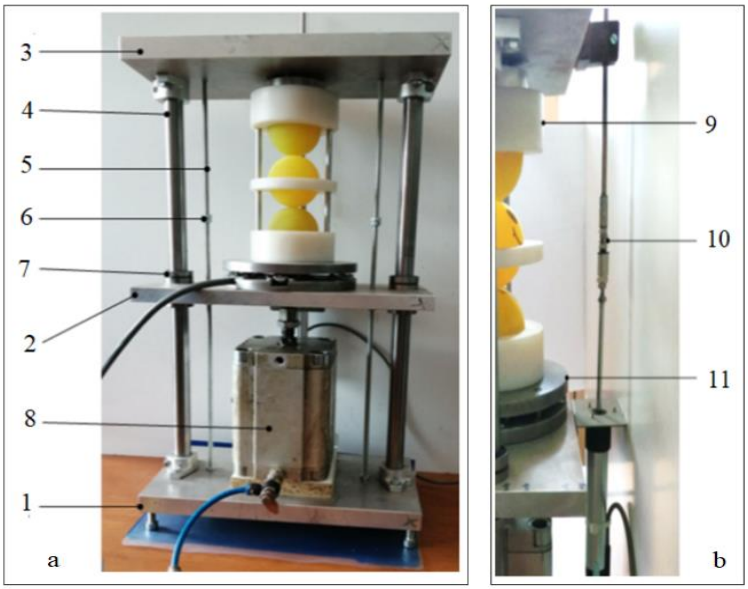

Figure 1. Test rig for compresional testing of rubber spheres. a) Front view b) Side view.
(1. Fixed base plate, 2. Movable intermediate plate, 3. Fixed upper plate, 4. Guide columns, 5. Safety rods, 6. Safety stop, 7. Ball bearing guide bushings, 8. Pneumatic cylinder, 9. Spheres support and guidance device, 10. Displacement transducer, 11. Force transducer)

As can be seen from Figure 1, between the upper plate and the movable intermediate plate, the assembly of spheres to be tested is mounted; spheres are positioned in a special device in order to align their centers on the same normal direction to the parallel surfaces of the plates.

Each sphere into the guidance device is held in the appropriate position relative to the other spheres due to the two mini-columns, which allows the relative linear displacement of the tested spheres.

Various types of guidance devices were built to support and guide the spheres, depending on the number of spheres used in the experiment (two or three spheres), the size of the used spheres (diameters of 42.35 mm and 54.4 mm, respectively).

Also, the guidance devices differ in terms of how the spheres rest into the supports. The spheres are placed into cylindrical cavities with a plane surface in the bottom part, then into hemispherical cavities of the guidance parts that copy spheres surfaces, and, finally, into supports with combined shapes (one in cavity with a plane surface in the bottom part and one in hemispherical cavity). In the case of contact between three spheres, arranged with collinear centers in the direction of load application, the device includes an additional guide ring for the intermediate sphere, also guided by the guidance mini-columns of the support and guidance device.

The displacement of the movable plate causes the spheres placed into the supports of the guidance device to compress or decompress, as the lower support of the device is placed on the movable plate, and moves with it. Thus, after the moment when the upper side of the device for supporting and guiding the spheres comes into contact with the fixed upper plate, the displacement of the movable plate is equivalent to the movement of the lower support part of the device and to the deformation of the spheres.

The value of the deformation force is measured using a resistive force transducer, the maximum measurable value of the force being F_{max}=1500 N. This transducer works on the basis of the tensor-resistive effect, which consists in changing the electrical resistance depending on the mechanical load, by changing the length, section and electrical resistivity of strain gauge type transducers. It uses four gauge transducers, configured in the form of a complete Wheatstone bridge, being adapted from a weighing scale, with an accuracy of 1%.

The value of the deformation is measured using a MIRAN KPF 75 resistive linear displacement transducer. It outputs an electrical signal that depends on the amount of displacement of a mobile element compared to a fixed position taken as a reference.

The measuring range of the transducer is 0 mm ~75 mm. Both limits have 2 mm buffer stroke and the accuracy is 0.25% ~ 0.08%.

The recorded data are transferred to a LabJack U-12 acquisition board and then transmitted via a data cable to a computer, where are stored.

3. Results and discussions

3.1. Results obtained from experiment

The recorded data were processed and graphs were created for their interpretation and analysis. For a clearer representation of the experimental results, a symbolization and a notation system was established, as follows: the general form of the experiment codification is 2(3)bM(m)(gg, pg, pp)15(25)a(b), where: 2(3) - number of balls (2 - two balls, 3 - three balls), b - balls; M(m) - sphere diameter category (M=54.4 mm, m=42.35 mm), g – sphere supported into cylindrical cavities with a plane surface in the bottom part, p - sphere supported in hemispherical cavities, a(b) - experiment number under identical conditions, 15(25) - maximum imposed deformation (mm), F(N) - deformation force, d(mm) - total deformation.

To perform the experiments, two spheres were initially used, which were placed into cylindrical cavities with a plane surface in the bottom part supports, then in hemi-spherical support and, finally, in combined supports (one flat-bottomed support and one hemi-spherical support). The maximum deformations, initially established, were 25 mm (Figure 2) and then 15 mm (Figure 3). Then, the same procedure was applied for three spheres and the force-deformation diagrams were drawn, and the results can be seen in Figures 4 and 5.

A comparison was made between the cumulative force-deformation diagrams for two spheres and a maximum deformation of 25 mm and 15 mm (Figure 6), then, for three spheres and a maximum deformation of 25 mm and 15 mm (Figure 7). It was then plotted a synthesis of all experimental results,

for two and three spheres, in all three modes of supporting them that are specified previously, for a maximum initially established deformation of 25 mm and 15 mm, respectively (Figure 8).

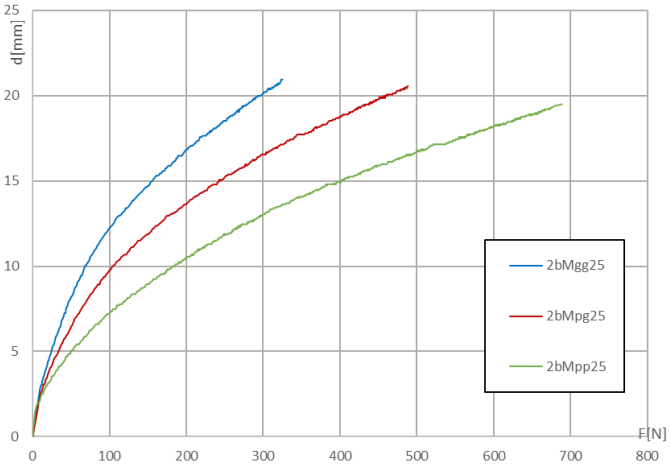

Figure 2. Cumulative results for two spheres (gg, pg and pp), maximum deformation of 25 mm

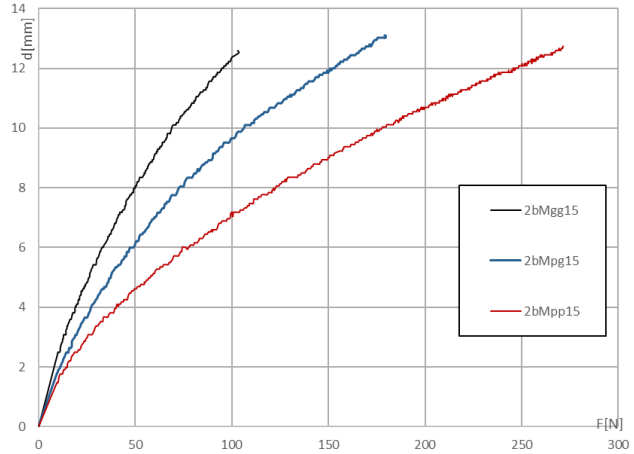

Figure 3. Cumulative results for two spheres (pp, pg and gg), maximum deformation of 15 mm

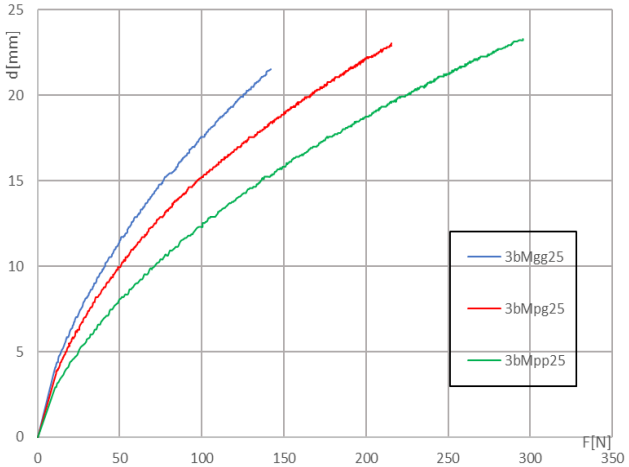

Figure 4. Cumulative results for three spheres (gg, pg, pp), maximum deformation 25 mm

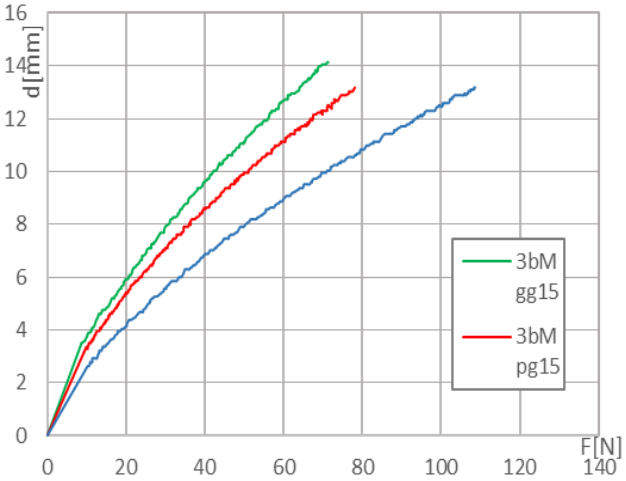

Figure 5. Cumulative results for three spheres (gg, pg, pp), maximum deformation of 15 mm

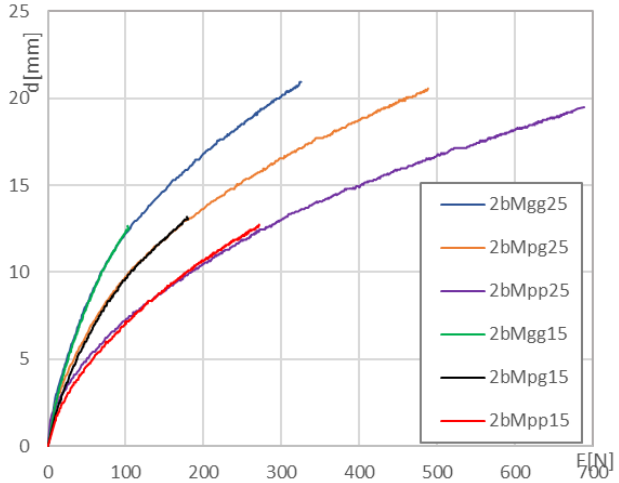

Figure 6. Comparison of force/deformation curves for two spheres (gg, pg, pp), maximum deformations of 15 mm and 25 mm

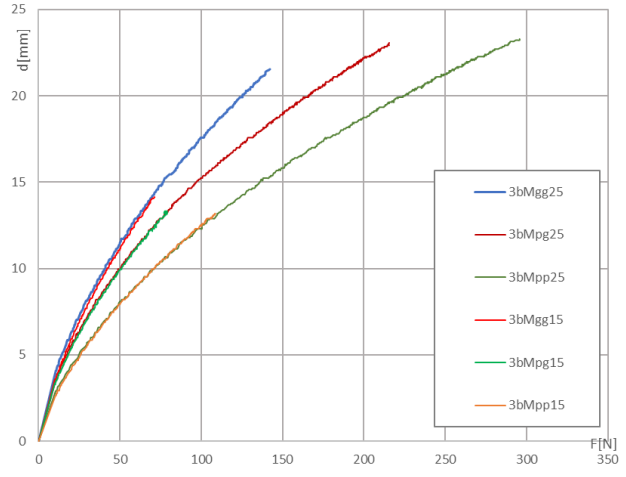

Figure 7. Comparison of force/deformation curves for three spheres (gg, pg, pp), maximum deformations of 15mm and 25mm

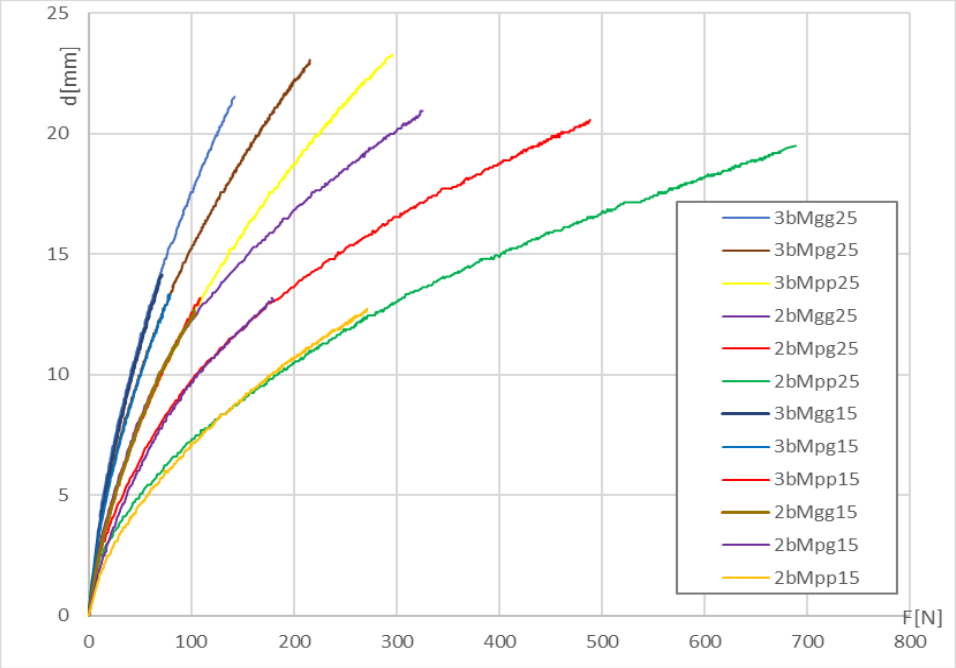

Figure 8. Synthesis of experimental data for three spheres and two spheres (gg, gp, pp) at maximum deformation of 25mm and 15mm

After performing the experiments, analyzing figures 2-8, the following conclusions can be drawn:

- the rubber spheres, tested in the experiment, had a non-linear-elastic deformation behavior, in accordance with literature [7, 8];
- the deformation curves are different, depending on the manner that the spheres are supported: both supports into cylindrical cavities with a flat bottom end (gg), a cylindrical cavity with a flat bottom end and a cavity with a hemi-spherical shape (pg), both cavities with a hemi spherical shape (pp), respectively. This is normal because the equivalent contact curvature differs from a case to the other case;
- there is a good correspondence between the force/deformation characteristic curves for both, a two-sphere system and a three-sphere system, regardless of the support mode used (in flat-bottomed supports, in hemispherical supports and combined), for the experiments with the initially established maximum deformations of 25 mm and 15 mm (Figures 6-8);
- repeating the experiment under identical conditions give good results in terms of repeatability, obtaining small scatters of the measured values, regardless of whether the experiment was performed for two spheres or for three spheres;
- for the same number of spheres and the same force value, the deformation is different, depending on the type of contact between the bodies in contact; its value increases with the number of sphere-sphere contacts and sphere-rigid flat surface contacts.

The evaluation of the deformation cannot be done directly, using classic calculation methods, such as Hertz's formula, because the Young's modulus of elasticity does not have a constant value during loading, and these formulas are based on the principle of superposition of effects, which can no longer be applied when Young's modulus of elasticity is not constant. In this case, the simplest way to determine the deformation is numerically, if the material characteristics are known.

3.2. Numerically obtained results

In order to validate the experimental results and the methodology presented above, a numerical simulation of the rubber sphere on a steel half-space contact was conducted.

Romanu [9] showed that, for hyperelastic materials, such as synthetic rubbers, a Mooney-Rivlin model can be used to simulate the rubber-like materials' behavior. The form of this model involves two constants, C_{10} and C_{01}.

To determine these constants, a simple methodology was proposed by Krmela and collaborators [10]. They experimentally determined the hardness of the hyperelastic material, measured on the Shore A scale, and using this value, they calculated the two constants, for the Mooney-Rivlin model.

It was applied a similar method, such as described in [10], and the rubber hardness was experimentally determinated using a hardness determination device (Shore A hardness tester), as can be seen in Figure 9. A set of five measurements in different points was carried out and an average value of 36 Shore A hardness was calculated.

According to the before mentioned article, the transverse elastic modulus is calculated with the formula:

$$G = 0.086 \cdot 1.045^{A} = 0.4194 \text{ MPa} \quad (1)$$

and the values of coefficients C_{10} and C_{01} are obtained:

$$C_{10} = \frac{G}{2} = 0.21 \text{ MPa}$$

and

$$C_{01} = 0.2\, C_{10} = 0.042 \text{ MPa}.$$

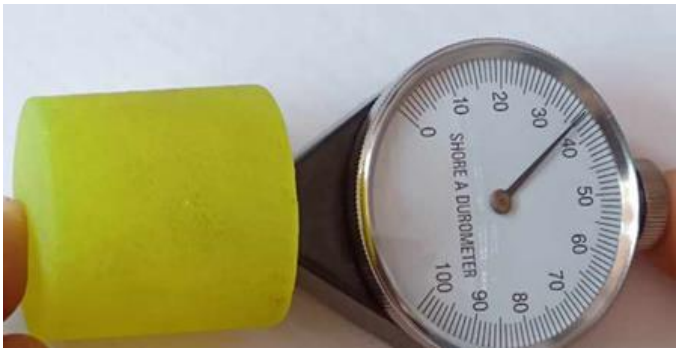

Figure 9. Hardness measurement

Knowing the values of the coefficients C_{10} and C_{01}, a constitutive model of the rubber was carried out. The sphere-plane contact was modeled, for a synthetic rubber sphere and a steel body with a flat surface (Figure 10).

Considering the symmetry character of the modeled body, a 2D model is run, using also the sphere was modeled by a quarter of a circle and the steel body with the flat surface was modeled by a square, considered quasi-rigid, because the modulus of elasticity of steel is five orders of magnitude higher than that of rubber and the steel body deforms much less compared to rubber. The discretization was done with different numbers of elements for the sphere part and for the conjugate part with a flat surface, as follows: for the sphere – 8274 elements and 8640 nodes, and for the conjugate part with a flat surface – 100 elements and 121 nodes (Figure 11). The planar character of the model imposes to restrict the movement of the points outside the plane.

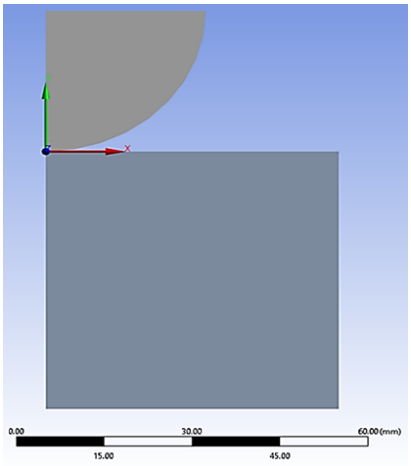

Figure 10. Rubber sphere geometry model on flat surface

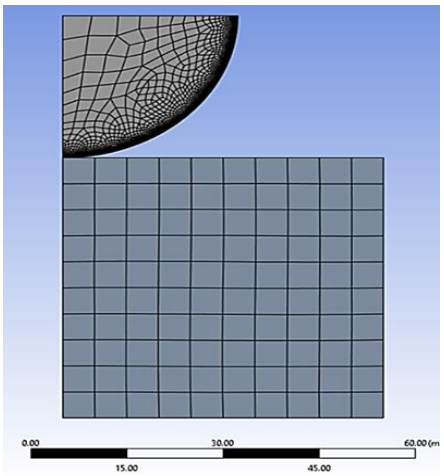

Figure 11. Discretization of bodies in contact

In the numerical model, the steel body was fixed in the lower part and the upper border of the sphere. The sphere model was subjected to a maximum imposed deformation of 12 mm, which is aproximatelly the equivalent of half the deformation of a contact between two whole spheres supported in spherical cavities, where it is considered that the deformation is only resulted from those of the free hemi-sphere. For the points on the vertical border of the sphere model, passing through the center of the sphere, the lateral movement was restricted.

The numerical model was solved using Ansys FEM software. Images of the total deformations of the two bodies in contact were obtained. The total deformations of the rubber sphere in contact with the rigid flat surface are represented in Figure 12.

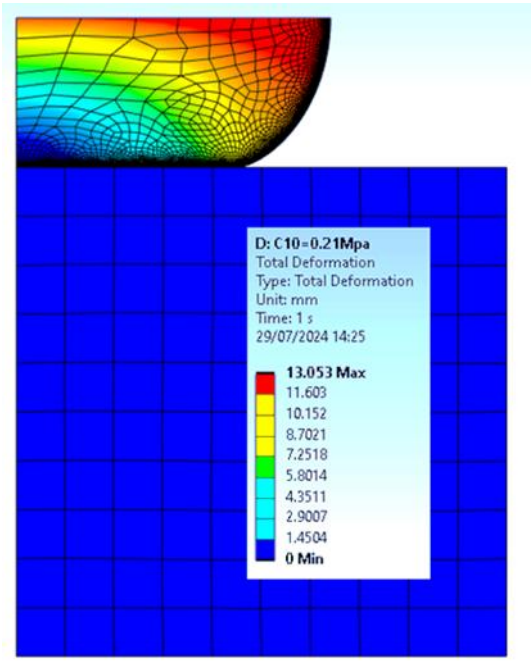

Figure 12. Distribution of total deformations of the rubber sphere in contact with the rigid flat surface, for a maximum imposed deformation of 12 mm

After solving the numerical model using finite elements method (FEM), the experimental curve for the sphere-plane deformation and the numerical curve for the similar situation with the rubber

constitutive model experimentally determined and the imposed approach of 12 mm were plotted on the same graph (Figure 13).

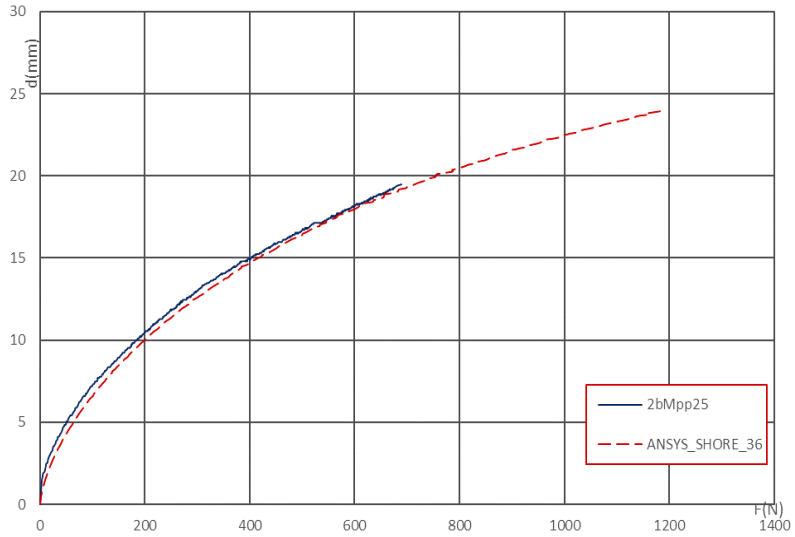

Figure 13. Comparison of experimental and numerical curves for two spheres with diameter of 54.4 supported in hemispherical cavities with initially established maximum deformations 25 mm

This figure shows a good correspondence between the experimentally obtained results and those numerically obtained.

4. Conclusions

Following the numerical modeling performed using the Ansys software, the following can be concluded.

The present paper highlights two ways of evaluating the deformation of spheres from hyperelastic materials, experimentally and numerically, the second way starting from the determination of the Mooney-Rivlin constants, specific to the material based on the Shore A hardness measurement of the material hardness.

The way to evaluate the mechanical characteristics of the material, namely the determination of the Mooney-Rivlin constants, is simple, effective and valid.

Modeling the axisymmetric contact as a quarter, through finite elements, is an elegant method of calculation because it uses a lower number of finite elements to obtain the numerical result and, implicitly, an important saving of resources is made.

The good correspondence between the experimental curve and numerical results in the range of studied values, validates both the numerical method and the experimental method.

Numerical modelling presented for determing the load – deformation correlation, based on experimental evaluation of the rubber hardness is satisfactory for design estimation of sphere behavior under compression load.

References

1.TREALOR, L., *The physics of rubber elasticity,* Clarendon press Oxford University Press 1975.
2.HIBBELER, R.C., Statics and Mechanics of Materials, Prentice Hall, 2014.
3.***https://www.fizichim.ro/docs/chimie/clasa10/capitolul2-hidrocarburi/II-4-alcadiene/II-4-3-cauciucul-natural-si-artificial/, accessed in 01.10. 2024.

4.KATSAMAKAS, A.A., BELSER, G., VASSILIOU, M.F., 2022, *Experimental investigation of a spherical rubber isolator for use in low income countries,* Engineering Structures, Vol. 250, 113522, ISSN 0141-0296, Elsevier, https://doi.org/10.1016/j.engstruct.2021.113522.
5.SÎRGHIE, E., MUSCĂ, I., ROMÂNU, I., IC 2021, *Experimental Study on Loading-Unloading RubberSpheres Deformation.* Tehnomus Journal, New Technologies and Products in Machine Manufacturing Technologies, no. 28, 57-63.
6.MUSCĂ, I., SÎRGHIE, E., MARCHITAN, M., *About local and volume deformation of rubber spheres*, ROTRIB 2024 – The 15th International Conference on Tribology, Bucharest, Romania, 2024.
7.TATARA, Y., 1991, On the Compresion of the Elastic Rubber Sphere over a Wide Range of Displacements, Part 1: Theoretical Study, Journal of Engineering Materials Technology, 285-291, Vol. 3, doi.10.1115/1.2903407. ISSN 0094-4289.
8.DIACONESCU, E., GLOVNEA, M., CIUTAC, F., 2009, *Circular Contact of Incompressible - Nonlinear Elastic Bodies*, Proceedings of the ASME/STLE International Joint Tribology Conference, 19-21 octombrie.
9.ROMÂNU, I.C., *End effect in linear contact between nonlinear elastic material bodies*, -PHD thesis, 2014. Suceava (in Romanian).
10.KRMELA, J., ARTYUKHOV, A., KRMELOVÁ, A., POZOVNYI, O., 2021, *Determination of material parameters of rubber and composites for computational modeling based on experiment data,* Journal of Physics: Conference Journal of Physics: Conference Series 1741, 012047, doi 10.1088/1742-6596/1741/1/012047.

Manuscript received: 25.08.2024